



Universiteit
Leiden
The Netherlands

Global control of development and antibiotic production by nutrient-responsive signalling pathways in *Streptomyces*

Swiatek, M.A.

Citation

Swiatek, M. A. (2012, November 29). *Global control of development and antibiotic production by nutrient-responsive signalling pathways in Streptomyces*. Retrieved from <https://hdl.handle.net/1887/20203>

Version: Not Applicable (or Unknown)

License: [Leiden University Non-exclusive license](#)

Downloaded from: <https://hdl.handle.net/1887/20203>

Note: To cite this publication please use the final published version (if applicable).

Cover Page



Universiteit Leiden



The handle <http://hdl.handle.net/1887/20203> holds various files of this Leiden University dissertation.

Author: Swiatek, Magdalena Anna

Title: Global control of development and antibiotic production by nutrient-responsive signalling pathways in *Streptomyces*

Issue Date: 2012-11-29

Chapter III

Functional analysis of the *N*-acetylglucosamine metabolic genes of *Streptomyces coelicolor* and role in the control of development and antibiotic production

Magdalena A. Świątek, Elodie Tenconi, Sébastien Rigali and Gilles P. van Wezel

Journal of Bacteriology (2012) 194(5):1136-44

Abstract

N-acetylglucosamine, the monomer of chitin, is a favored carbon and nitrogen source for streptomycetes. Its intracellular catabolism requires the combined actions of the *N*-acetylglucosamine-6-phosphate (GlcNAc-6P) deacetylase NagA and the glucosamine-6-phosphate (GlcN-6P) deaminase/isomerase NagB. GlcNAc acts as a signalling molecule in the DasR-mediated nutrient sensing system, activating development and antibiotic production under poor growth conditions (*famine*), while blocking these processes under rich conditions (*feast*). In order to understand how a single nutrient can deliver opposite information according to the nutritional context, we carried out a mutational analysis of the *nag* metabolic genes *nagA*, *nagB* and *nagK*. Here we show that the *nag* genes are part of the DasR regulon in *S. coelicolor*, which explains their transcriptional induction by GlcNAc. Most likely as the result of the intracellular accumulation of GlcN-6P, *nagB* deletion mutants fail to grow in the presence of GlcNAc. This toxicity can be alleviated by the additional deletion of *nagA*. We recently showed that in *S. coelicolor*, GlcNAc is internalized as GlcNAc-6P via the phosphoenolpyruvate-dependent sugar phosphotransferase system PTS. Considering the relevance of GlcNAc for the control of antibiotic production, improved insight into GlcNAc metabolism in *Streptomyces* may provide new leads towards biotechnological applications.

INTRODUCTION

Streptomyces are Gram-positive, soil-dwelling mycelial bacteria that have a complex life cycle that starts with the germination of a spore, which then grows out to form a branched mycelium of vegetative hyphae. The multicellular mycelial life style of streptomyces makes these organisms unique among bacteria, whereby connected compartments are formed that are separated by cross-walls. When morphological differentiation is initiated a so-called aerial mycelium is produced, and the erected aerial hyphae eventually form chains of spores (Flårdh & Buttner, 2009; Redington & Chater, 1997). Streptomyces are prolific producers of natural products, producing some fifty percent of all known antibiotics as well as many anticancer, antifungal and immunosuppressant agents. The production of these so-called secondary metabolites is part of the developmental program, roughly coinciding with growth cessation and the onset of sporulation (Bibb, 2005; van Wezel & McDowall, 2011).

As saprophytic soil bacteria, streptomyces utilize naturally occurring polysaccharides such as chitin, xylan and cellulose as carbon sources. *N*-acetylglucosamine, the monomer of chitin, is a preferred carbon and nitrogen source for streptomyces, and the related metabolite glutamate is preferred over glucose (Nothaft *et al.*, 2003b; van Wezel *et al.*, 2006). Chitin is one of the most abundant polysaccharides on earth and found in among others the cuticles and shells of insects and crustaceans and within the cell wall of fungi, and to utilize this polysaccharide streptomyces have an extensive chitinolytic system (Cohen-Kupiec & Chet, 1998; Schrempf, 2001). *N*-acetylglucosamine (GlcNAc) is a substrate in *Streptomyces coelicolor* for transport via the phosphoenolpyruvate-dependent phosphotransferase system (PTS; reviewed in Brückner & Titgemeyer, 2002). During PTS-mediated carbon source uptake, a phosphoryl group is transferred from phosphoenolpyruvate to the general phosphotransferase enzyme I (EI; encoded by *ptsI*), from there to HPr (encoded by *ptsH*) and further onto Enzyme IIA (EIIA^{Crr}; encoded by *crr*) and finally Enzyme IIB (NagF) (Nothaft *et al.*, 2003b; Nothaft *et al.*, 2010). NagF phosphorylates incoming via the permease IIC (NagE2) GlcNAc to form *N*-acetylglucosamine-6-phosphate (GlcNAc-6P). Removal of any of the general PTS components EI, EIIA or HPr blocks development (Rigali *et al.*, 2006). An alternative route for the internalization of monomeric GlcNAc exists in *Streptomyces olivaceoviridis* and probably many other streptomyces, namely

via the ATP-binding cassette (ABC) transporter NgcEFG, which imports both *N*-acetylglucosamine and its disaccharide *N,N'*-diacetylchitobiose (GlcNAc)₂ with similar affinities (Wang *et al.*, 2002; Xiao *et al.*, 2002). (GlcNAc)₂ is also imported via the ABC sugar transporter DasABC (Colson *et al.*, 2008; Seo *et al.*, 2002).

We previously demonstrated that GlcNAc is an important signalling molecule for streptomycetes and a major decision point towards the onset of development and antibiotic production (Rigali *et al.*, 2006; Rigali *et al.*, 2008). When GlcNAc accumulates under rich growth conditions (*feast*) it promotes growth, thereby blocking developmental processes, while under poor nutritional conditions (*famine*) the accumulation of GlcNAc promotes development and antibiotic production (Rigali *et al.*, 2008; van Wezel *et al.*, 2009). Under famine conditions, a complete signalling pathway was proposed from GlcNAc uptake to the onset of antibiotic production, whereby the pleiotropic GntR-family transcriptional regulator DasR controls the genes for GlcNAc transport and metabolism and for antibiotic synthesis (Rigali *et al.*, 2006; Rigali *et al.*, 2008). Glucosamine-6-phosphate (GlcN-6P) is a key molecule in this signalling cascade, and acts as an allosteric effector preventing DasR DNA-binding ability. This results in the loss of transcriptional repression of specific activator genes for antibiotic production, including *actII*-ORF4, encoding the pathway-specific activator for actinorhodin (Act) production, and *redZ*, for the response regulator RedZ that activates prodiginine (Red) production. DasR also represses the *cpk* gene cluster for the cryptic polyketide Cpk, but this effect is probably indirect (van Wezel & McDowall, 2011). Under feast conditions, the molecular mechanism of how GlcNAc blocks sporulation and antibiotic production is still unknown. Non-phosphorylation of key developmental proteins by global PTS components (EI, HPr, and EIIA^{Cr}) upon GlcNAc sensing is so far the only realistic hypothesis proposed (Colson *et al.*, 2008; Rigali *et al.*, 2006).

As can be gleaned from extensive studies of aminosugar metabolism in other bacteria, the signalling molecule GlcN-6P is produced from *N*-acetylglucosamine-6-phosphate by a GlcNAc-6P deacetylase (NagA), and is then converted by a GlcN-6P deaminase (NagB) to fructose-6-phosphate (Fru-6P), which enters the glycolytic pathway (Alvarez-Anorve *et al.*, 2005; Plumbridge & Vimr, 1999; Vogler & Lengeler, 1989). To better understand the aminosugar-mediated signalling pathway in streptomycetes, dissection of GlcNAc metabolism in these organisms is required. In this work we analyze

the GlcNAc-metabolic pathway and specifically block one or more steps of GlcNAc utilization via directed deletion mutants. This allows us to provide a first assessment as to how the flux of GlcNAc influences the global regulatory routes that control *Streptomyces* development and antibiotic production.

MATERIALS AND METHODS

Bacterial strains and growth conditions

Bacterial strains and plasmids are listed in Table 1 and Supplemental Table S1, respectively. *Escherichia coli* JM109 (Sambrook *et al.*, 1989) and ET12567 (Kieser *et al.*, 2000) were used for routine cloning procedures and for extracting non-methylated DNA, respectively. *Streptomyces coelicolor* A3(2) M145 was the parent for all mutants described in this work. All media and routine *Streptomyces* techniques are described in the *Streptomyces* manual (Kieser *et al.*, 2000). Cells of *E. coli* were grown in Luria–Bertani broth (LB) at 37°C. Phenotypic characterization of *Streptomyces* mutants was carried out on minimal media (MM) and on R5- (-glucose) agar plates and in liquid NMMP or MM cultures (Kieser *et al.*, 2000) with 1% of carbon sources as indicated. SFM (soy flour mannitol) agar plates were used to prepare spore suspensions.

Table 1. Strains of *Streptomyces coelicolor* A3(2) described in this study.

Strain	Genotype ^a	Reference
M145	prototrophic SCP1 ⁺ SCP2 ⁻	(Kieser <i>et al.</i> , 2000)
GAM1	M145 <i>nagA::aacC4</i> , Apr ^R	this work
GAM2	M145 <i>nagB::aacC4</i> , Apr ^R	this work
GAM3	M145 <i>nagK::aacC4</i> , Apr ^R	this work
GAM4	M145 Δ <i>nagA</i> ^{IFD}	this work
GAM5	M145 Δ <i>nagB</i> ^{IFD}	this work
GAM6	M145 Δ <i>nagK</i> ^{IFD}	this work
GAM7	M145 Δ <i>nagKA::aacC4</i> , Apr ^R	this work
GAM8	M145 Δ <i>nagKA</i> ^{IFD}	this work
GAM9	M145 Δ <i>nagB</i> ^{IFD} <i>nagA::aacC4</i>	this work
GAM10	M145 Δ <i>nagKA</i> ^{IFD} <i>nagB::aacC4</i>	this work
GAM12	GAM4 + pGAM5	this work
GAM13	GAM5 + pGAM6	this work

^a IFD, in-frame deletion mutant; Apr^R, apramycin resistant.

Plasmids and constructs

All constructs described in this work are listed in Supplemental Table S1 and oligonucleotides in Supplemental Table S2.

Constructs for creating gene-replacement and in-frame deletion mutants

The strategy for creating knock-out mutants is based on the unstable multi-copy vector

pWHM3 (Vara *et al.*, 1989) as described previously (van Wezel *et al.*, 2005). For the deletion of *nagA*, the -1365/+6 and +1133/+2484 regions relative to the start of *nagA* were amplified by PCR, using primer pairs nagALF-1365 and nagALR+6 and nagARF+1133 and nagARR+2484 respectively. Fragments were cloned into pWHM3, and the engineered *Xba*I site was used for insertion of the apramycin resistance cassette *aacC4* flanked by *loxP* sites between the flanking regions. The presence of the *loxP* recognition sites allows the efficient removal of the apramycin resistance cassette following the introduction of a plasmid pUWLcre expressing the Cre recombinase (Fedoryshyn *et al.*, 2008; Khodakaramian *et al.*, 2006). The constructed plasmid was called pGAM1. Using essentially the same strategy as for pGAM1, we constructed the knock-out plasmids pGAM2 and pGAM3 for the single gene replacement of *nagB*, *nagK* respectively. pGAM2, contains the -1185/+6 and +770/+1918 regions relative to the start of *nagB*, and pGAM3 the -1450/+6 and +963/+2570 regions relative to the start of *nagK*. Plasmid pGAM4 for the in-frame deletion of *nagKA* contains the upstream -1450/+6 region of *nagK* and downstream +1133/+2484 region of *nagA*, which were amplified by PCR, using primer pairs nagKLF-1450 and nagKLR+6 and nagARF+1133 and nagARR+2484, respectively. The *nagAB* (GAM9) double mutant was constructed by replacing *nagA* by the apramycin cassette in the *nagB*^{IFD} mutant GAM5. GAM8 was used as the parent for *nagKAB* triple mutant GAM10, following replacement of *nagB* by the apramycin resistance cassette.

To analyse correctness of the mutants, PCRs were done on mycelium from liquid-grown MM cultures, with oligonucleotides pairs nagA_FOR-198 and nagA_REV+1417 for *nagA* and nagBFOR-336 and nagB_REV+1098 for *nagB*.

For complementation of the *nag* mutants the low copy vector pHJL401 (Larson and Hershberger, 1986) harboring the corresponding *nag* gene and promoter region (nt positions -454/+796 relative to the start of *nagB*; fragment -512/+2262 relative to the start of *nagK* were used to complement *nagK* and *nagA*) was used.

Antibiotic production

Quantification of prodiginines and actinorhodin was performed as described (Kieser *et al.*, 2000), and corrected for biomass (wet weight). Values were normalized against the parental strain M145 (set to 100%). Cultures were grown on R2YE agar plates overlaid

with cellophane discs to allow separation of biomass and spent agar.

Production and purification of DasR

Production and purification of His₆-tagged DasR was based on the protocol described previously (Colson *et al.*, 2007; Mahr *et al.*, 2000) with several modifications. *Escherichia coli* BL21 Rosetta (DE3) cells carrying pFT240 (Rigali *et al.*, 2004) were grown at 37°C in 250 ml LB medium containing 100 µg/ml of ampicillin until the culture reached an OD₆₀₀ of 0.6. Production of His₆-tagged DasR was induced by addition of 1 mM isopropyl thio-β-d-galactoside (IPTG) during 3h. Cells were collected by centrifugation, and ruptured by sonication in lysis buffer (100 mM phosphate buffer pH 8 ; 250 mM NaCl ; 30 mM imidazole ; 0.1% Triton). Soluble proteins were loaded onto a pre-equilibrated Ni²⁺-NTA-agarose column (5 ml bed volume). His₆-tagged DasR eluted at around 200 mM imidazole and fractions containing the pure protein were pooled and dialysed overnight at 4°C against EMSA buffer (see below).

Electromobility gel shift assays

EMSAs on double-stranded oligonucleotides were performed using Cy5-labelled *dre* probes (0.25 µM final concentration) and His₆-tagged DasR (between 1.75 and 2.5 µM final concentration) in a total reaction volume of 50 µl. All reactions were carried out in EMSA buffer (10 mM Tris-Cl pH 7.5, 1mM DTT, 0.25 mM CaCl₂, 0.5 mM MgCl₂, 50 mM KCl, and 2% glycerol) containing a 100-fold excess of non-specific DNA (salmon sperm DNA). After 15 min of incubation at room temperature, reaction mixtures were loaded into a 1% (w/v) agarose gel. Bound and unbound probes were separated by gel electrophoresis at room temperature and fluorescent DNA was visualised using a Typhoon Trio+ Variable Mode Imager. Oligonucleotides (see Table S2) used to generate 40 bp double-stranded DNA probes for EMSAs were taken from the upstream regions of *dasA* (*dre^{dasA}*), *nagB* (*dre^{nagB}*), and the *nagKA* operon (*dre^{nagKA}*). The *cis*-acting element OP1 of the gene for the *Bacillus licheniformis* β-lactamase repressor BlaI was used as negative control.

RNA isolation and RT-PCR

For transcript analysis, RNA was isolated from liquid cultures of *S. coelicolor* M145 or

the *dasR* mutant. Mycelium was grown in NMMP and induced by addition of 50 mM GlcNAc at OD~0.2. Samples were taken before induction (t = 0') and 30 min after induction (t = 30'). RNA isolation and semi-quantitative RT-PCR was carried out twice as described previously (Birko et al., 2009). 200 ng of RNA was used for each reaction (concentration was assessed using a Nanodrop® spectrophotometer). Quantification was done using a Bio-Rad FX molecular imager with Quantity One software (Bio- Rad). Oligonucleotides used for RT-PCR are presented in Supplemental Table S2.

Stereo microscopy

Strains were grown on MM and R5- agar plates supplemented either with mannitol or GlcNAc for five days. The mutants were imaged using a Zeiss Lumar V12 stereomicroscope.

Computer analyses

DNA and protein databank searches were performed using the BLAST server of the National Center for Biotechnology Information at the National Institute of Health, Bethesda, MD, USA (<http://www.ncbi.nlm.nih.gov>) and the *S. coelicolor* genome page services (<http://strepdb.streptomyces.org.uk/>). Alignments were generated with CLUSTALW available at <http://www.ebi.ac.uk/clustalw>. Regulon predictions were performed using PREDetector (Hiard *et al.*, 2007). The general information about amino sugar metabolic pathway of *S. coelicolor* was found in the KEGG database (http://www.genome.jp/kegg-bin/show_pathway?map00520a).

RESULTS

In silico identification of the GlcNAc utilization genes in *S. coelicolor*

The genetic environment of the *nag* metabolic genes on the *S. coelicolor* chromosome and the predicted gene products are presented in Fig. 1A. The *nagK* (SCO4285) and *nagA* (SCO4284) genes have overlapping start and stop codons, and encode *N*-acetylglucosamine kinase NagK and *N*-acetylglucosamine-6P deacetylase NagA, respectively. The NagA and NagK proteins show 34.5% and 37.2% amino acid sequence identity to the corresponding enzymes in *E. coli*, respectively. Downstream of the *nagKA* operon lies SCO4283, for a phosphofructokinase-like sugar kinase, and upstream lies SCO4286, which encodes an ABC-type sugar binding protein of unknown function. The *nagB* gene for glucosamine-6P-deaminase (SCO5236) lies immediately downstream of the *dasABCD* gene cluster involved in (GlcNAc)₂ uptake and degradation (Colson *et al.*, 2008; Saito *et al.*, 2007), and upstream of SCO5237 for a likely 3-ketoacyl-(acyl-carrier-protein) reductase. NagB shows 44.6% amino acid sequence identity with NagB from *E. coli*. The GlcNAc-related metabolic pathway of *S. coelicolor*, based on the KEGG database is shown in Fig. 1B.

Expression of *nagA* and *nagB* is induced by GlcNAc and repressed by DasR

Prior to assessing the effect of the inactivation of the *nag* genes on the GlcNAc-mediated signalling pathway in *S. coelicolor*, we first analyzed the GlcNAc-dependent control of the *nagA*, *nagB* and *nagK* genes. DasR is a global regulator of primary metabolism and antibiotic production, and is known to control among others the chitinolytic system in *S. coelicolor* (Colson *et al.*, 2007; Nazari *et al.*, 2011), as well as *nagB* (Rigali *et al.*, 2006). The latter has a DasR-responsive element or *dre* at position -68 upstream of *nagB* (tGTGGTtTAGACCAaT, *dre*^{*nagB*}), which has a 13 nt match to the *dre* consensus sequence (AGTGGTCTAGACCACT, *dre*^{*cons*}; (Rigali *et al.*, 2006)). Suggestively, the program PREDetector (Hiard *et al.*, 2007) also identified a *dre* element (AGaGGTCTAGtCCACT, *dre*^{*nagKA*}) at position -83 upstream of the *nagKA* operon that matches 14 out 16 nt to the *dre* consensus sequence. Furthermore, the computational prediction of the DasR regulon in five other streptomycetes revealed identical or similar *dre*-like sequences upstream of the respective *nagKA* and *nagB* orthologs, and the very high conservation suggests that these sites are true functional *cis*-acting elements. In

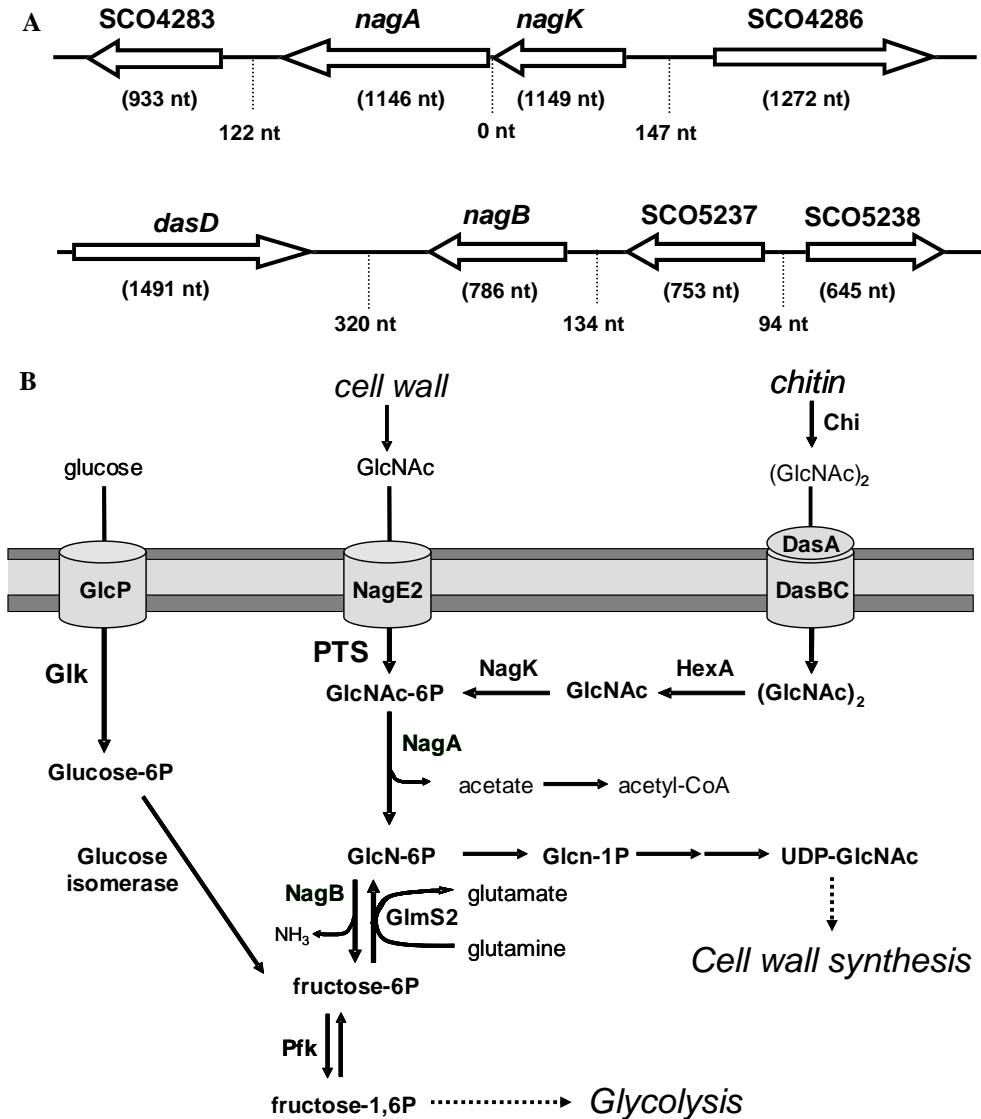


Figure 1. Genetic environment of the *nag* metabolic genes and GlcNAc-related primary metabolism.

A. Map of the genomic regions around the aminosugar utilization genes. *nagB* (SCO5236) is a single transcription unit, while *nagK* (SCO4285) and *nagA* (SCO4284) together form the *nagKA* operon. ORFs are indicated by open arrows. Lengths of the genes (in brackets below the genes) and intergenic regions (dotted line) are indicated. **B.** Aminosugar metabolism in *S. coelicolor* and connecting pathways. Annotation based on KEGG and experimental evidence. Arrows show direction of metabolism, and the responsible enzymes are depicted next to them. It is unknown whether GlcN-6P can be metabolized directly to GlcNAc-6P. Names and functions of the enzymes and the reactions they catalyze are listed in Table 2.

Table 2. Genes involved in GlcNAc transport and metabolism in *S. coelicolor* A3(2).

Name	Gene	Predicted function ^a
<i>crr</i>	SCO1390	Global PTS component EIIA ^{Crr}
<i>gdhA</i>	SCO4683	Glutamate dehydrogenase (EC 1.4.1.4) Glu + H ₂ O + NADP ⁺ \rightleftharpoons 2-OG + NH ₃ + NADPH + H ⁺
<i>glmM</i>	SCO4736	Phosphoglucosamine mutase (EC 5.4.2.10) GlcN-1P \rightleftharpoons GlcN-6P
<i>glmS1</i>	SCO4740	glucosamine-fructose-6-phosphate aminotransferase (EC 2.6.1.16) Gln + Fru-6P \rightleftharpoons Glu + GlcN-6P
<i>glmS2</i>	SCO2789	glucosamine-fructose-6-phosphate aminotransferase (EC 2.6.1.16) Gln + Fru-6P \rightleftharpoons Glu + GlcN-6P
<i>glmU</i>	SCO3122	bifunctional N-acetylglucosamine-1-phosphate uridylyltransferase/ glucosamine-1-phosphate acetyltransferase (EC 2.7.7.23) UTP + GlcNAc-1P \rightleftharpoons 2P _i + UDP-GlcNAc (EC 2.3.1.157) Ac-CoA + GlcN-1P \rightleftharpoons CoA + GlcNAc-1P
<i>hexA</i>	SCO2758,	beta-N-acetylglucosaminidase (EC 3.2.1.52)
	SCO2786,	beta-N-acetylhexosaminidase (EC 3.2.1.52)
	SCO2943,	sugar hydrolase (EC 3.2.1.52)
	SCO4860	secreted hydrolase (EC 3.2.1.52) (GlcNAc) ₂ + H ₂ O \rightleftharpoons 2 GlcNAc
<i>nagA</i>	SCO4284	N-acetylglucosamine-6-phosphate deacetylase (EC 3.5.1.25); GlcNAc-6P + H ₂ O \rightleftharpoons GlcN-6P + OAc-
<i>nagB</i>	SCO5236	Glucosamine phosphate isomerase (EC 3.5.99.6); GlcN-6P + H ₂ O \rightleftharpoons Fru-6P + NH ₃
<i>nagE2</i>	SCO2907	PTS ^{GlcNAc} transmembrane component EIIC
<i>nagF</i>	SCO2905	PTS ^{GlcNAc} transmembrane component EIIB
<i>nagK</i>	SCO4285	N-acetylglucosamine kinase (EC 2.7.1.59) GlcNAc + ATP \rightleftharpoons GlcNAc-6P + ADP
<i>murA</i>	SCO2949	UDP-N-acetylglucosamine 1-carboxyvinyltransferase (EC 2.5.1.7) UDP-N-acetylglucosamine transferase (EC 2.5.1.7)
(<i>murA2</i>)	SCO5998	PEP + UDP-GlcNAc \rightleftharpoons uaccg + OP
<i>murB</i>	SCO4643	UDP-N-acetylenolpyruvoylglucosamine reductase (EC 1.1.1.158) UNAM + NADP ⁺ \rightleftharpoons uaccg + NADPH + H ⁺
<i>murQ</i>	SCO4307	N-acetylmuramic acid-6-phosphate etherase (EC 4.2.-.-) MurNAc-6P + H ₂ O \rightleftharpoons GlcNAc-6P + Lactate
<i>ptsH</i>	SCO5841	Global PTS component HPr
<i>ptsI</i>	SCO1391	Global PTS component EI

^a Abbreviations of metabolites: OAc⁻, acetate; AcCoA, acetyl coenzyme A; ADP, Adenosine Di-Phosphate; ATP, Adenosine Tri-Phosphate; (GlcNAc)₂, chitobiose; 2P_i, diphosphate; chitobiose, N,N'-diacetylchitobiose; Fru, fructose; Fru-6-P, fructose-6-phosphate; GlcNAc, N-acetyl-D-glucosamine; GlcNAc-1P, N-acetyl glucosamine 1-phosphate; GlcNAc-6P, N-acetyl glucosamine-D-6-phosphate GlcN, glucosamine; GlcN-1P, Glucosamine 1-phosphate; GlcN-6P, Glucosamine 6-phosphate; Gln, glutamine; Glu, glutamate; MurNAc-6P, N-Acetylmuramic acid 6-phosphate; NADP, nicotinamide adenine dinucleotide phosphate; NADPH, nicotinamide adenine dinucleotide phosphate (reduced form); OP, Orthophosphate; 2-OG, oxoglutarate; PEP, phosphoenolpyruvate; UDP-GlcNAc, Uridine diphosphate N-acetyl D-glucosamine; uaccg, UDP-N-acetyl -3-O-(1-carboxyvinyl)-D-glucosamine; UNAM, UDP-N-acetylmuramate.

order to validate our *in silico* predictions, electromobility gel shift assays (EMSAs) were performed *in vitro* using His₆-tagged DasR and a short double-stranded oligonucleotide centered on *dre*^{nagKA} and *dre*^{nagB}. Positive specific DasR-*dre* interactions were observed for both *dre* sequences as well as for another positive control (the *dre* upstream of *dasA*), while the negative control (the *cis*-acting element of *blaI* of *Bacillus licheniformis*) was not bound by DasR (Fig. 2A).

If the *nag* genes are repressed by DasR, it would follow that their expression should be at least partially independent of induction by GlcNAc in a *dasR* null mutant. To test this hypothesis, *S. coelicolor* M145 and its Δ *dasR* null mutant were grown in liquid NMMP medium until OD₆₀₀~0.2 followed by the addition of 25 mM GlcNAc. Mycelia were harvested for RNA preparation immediately before and 30 min after GlcNAc addition. Semi-quantitative RT-PCR on total RNA samples from the wild-type strain *S. coelicolor* M145 showed an induction of *nagA*, *nagK*, and *nagB* transcript levels by two-, three-, and five-fold, respectively following the addition of GlcNAc, while transcripts of the control *rspI* (for the ribosomal protein S9) were readily identified before and after induction and did not show significant induction (Fig. 2BC). In contrast, expression of the *nag* genes was already high in the *dasR* null mutant before induction, with similar transcript levels before and after the addition of GlcNAc (Fig. 2BC). This is consistent with induction of the *nagA*, *nagB* and *nagK* genes by GlcNAc and repression of these genes by DasR. The induction by GlcNAc most likely acts via the allosteric inactivation of DasR by the GlcNAc-derived metabolite GlcN-6P (Rigali *et al.*, 2006; Rigali *et al.*, 2008).

***nagA* and *nagB* gene-replacement and in-frame deletion mutants**

To study the effect of the accumulation of GlcNAc-related metabolites on growth, development and antibiotic production, null mutants were constructed for *nagA* and *nagB*. For this, we first replaced the entire coding region of *nagA* or *nagB* by the apramycin cassette (*aacC4*) flanked by *loxP* sequences and then removed the cassette to generate the respective in-frame deletion (IFD) mutants (see Materials and Methods section). For each experiment five transformants exhibiting the desired double-crossover phenotype (Apra^R Thio^S) were selected and verified by PCR as described in the Materials and Methods section. The mutants were designated GAM1 (*nagA*::*aacC4*), and GAM2

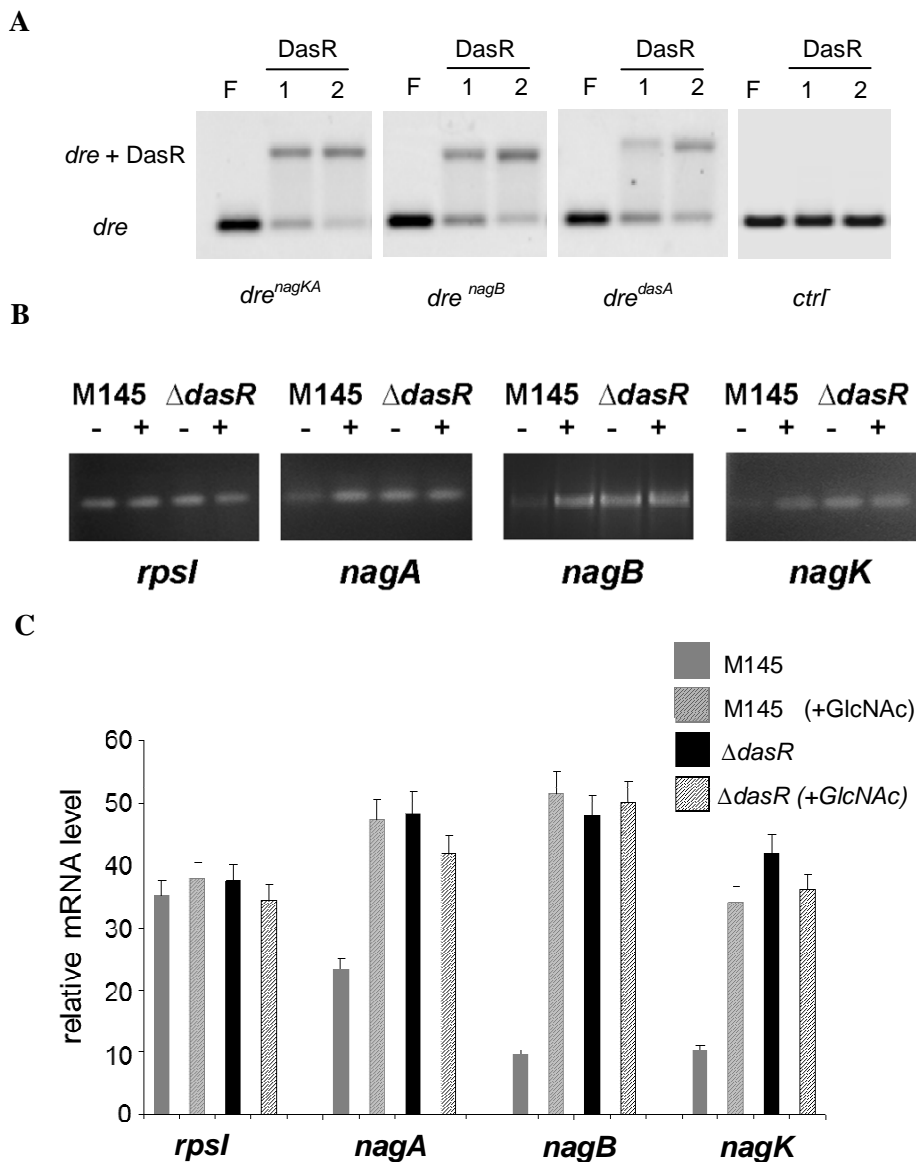


Figure 2. Direct transcriptional control of *nagKA* and *nagB* by DasR.

A. DasR binding to predicted *dre* upstream of *nagKA* and *nagB*. EMSAs were performed with pure DasR-His₆ and a 40 bp Cy5 double-stranded oligonucleotide probe centred on the DasR-responsive elements (*dre*) in the promoter regions of *nagKA* (*dre^{nagKA}*), *nagB* (*dre^{nagB}*), and *dasA* (*dre^{dasA}*, positive control), with short flanking sequences. The *cis*-acting element of *blaI* of *Bacillus licheniformis* was used as negative control (*ctrl*). **fp**, free probe (0.25 μ M of double stranded Cy5 labelled probe); **1** and **2**, DasR/*dre* binding reactions with 1.75 and 2.5 μ M of DasR-His₆, respectively; *dre*, DasR responsive element.

B. Induction of *nag* transcription by GlcNAc and control by DasR. Semi-quantitative RT-PCR was carried out on RNA isolated from the *dasR* null mutant or its parent *S. coelicolor* M145, grown in liquid mineral media (NMMP + mannitol) cultures immediately prior to (-) or 30 min after (+) the addition of 25 mM GlcNAc. The constitutive expression of *nagA*, *nagK* and *nagB* in *dasR* null mutants and their enhanced transcript levels in wild-type cells 30 min after induction, shows that the *nag* genes are repressed by DasR and induced by *N*-acetylglucosamine.

(*nagB::aacC4*) respectively. Following removal of the *aacC4* cassette by the Cre recombinase, in-frame deletion (IFD) mutants were obtained for *nagA* (designated GAM4) and *nagB* (GAM5). For all experiments both the apramycin resistant and the IFD mutants were analyzed. Considering that there were no phenotypic differences between them in terms of antibiotic production and development, from this point onwards we will only describe the results obtained for the IFD mutants unless stated otherwise. The *nagAB* double mutant GAM9 was created by replacing *nagA* by the apramycin cassette in the *nagB*^{IFD} mutant GAM5.

Effect of GlcNAc on growth of the *nagA* and *nagB* mutants in liquid-grown cultures

The addition of GlcNAc is expected to result in the accumulation of GlcNAc-6P in *nagA* mutants, and of GlcN-6P in *nagB* mutants (Fig. 1B). Growth of *nagB* mutants was analyzed in liquid mineral medium (NMMP) and compared to that of the parental strain *S. coelicolor* M145. While there was little difference in terms of growth on mannitol, *nagB* mutants failed to grow in the presence of GlcNAc. This is in line with the observed toxicity of the NagB substrate GlcN-6P in other bacteria (Bernheim & Dobrogosz, 1970; Plumbridge, 2009; White, 1968). Addition of mannitol did not restore growth, strongly suggesting that rather than the inability to utilize GlcNAc, it is toxicity of a GlcNAc-derived metabolite that prevents growth of *S. coelicolor* in the absence of *nagB* (Fig. 3A). To analyze if the sensitivity to GlcNAc prevails throughout growth or only occurs during the earliest growth phases (*i.e.* germination and very early vegetative growth), we monitored growth in NMMP supplemented with mannitol (1% w/v), followed by the addition of 25 mM GlcNAc at an OD₆₀₀ of 0.2 (early log phase) (Fig. 3B). Surprisingly, under these conditions the mutant strain had a similar growth rate as the parent, indicating that GlcNAc toxicity is alleviated once a certain amount of biomass has accumulated. To rule out an effect specifically on spore germination, spores of *S. coelicolor* M145 and its *nagB* null mutant GAM5 were allowed to germinate for 8h in

2xYT at 30°C and used as inoculum of liquid mineral media cultures. Despite the obvious emergence of germ tubes as well as many young vegetative hyphae, as assessed by phase-contrast microscopy, the germinated *nagB* mutant spores still failed to grow in the presence of GlcNAc (Fig. 3C). This illustrates that in the absence of the GlcN-6P deaminase activity of NagB, GlcNAc is toxic to young vegetative hyphae, but that this is alleviated once a threshold amount of biomass has been produced.

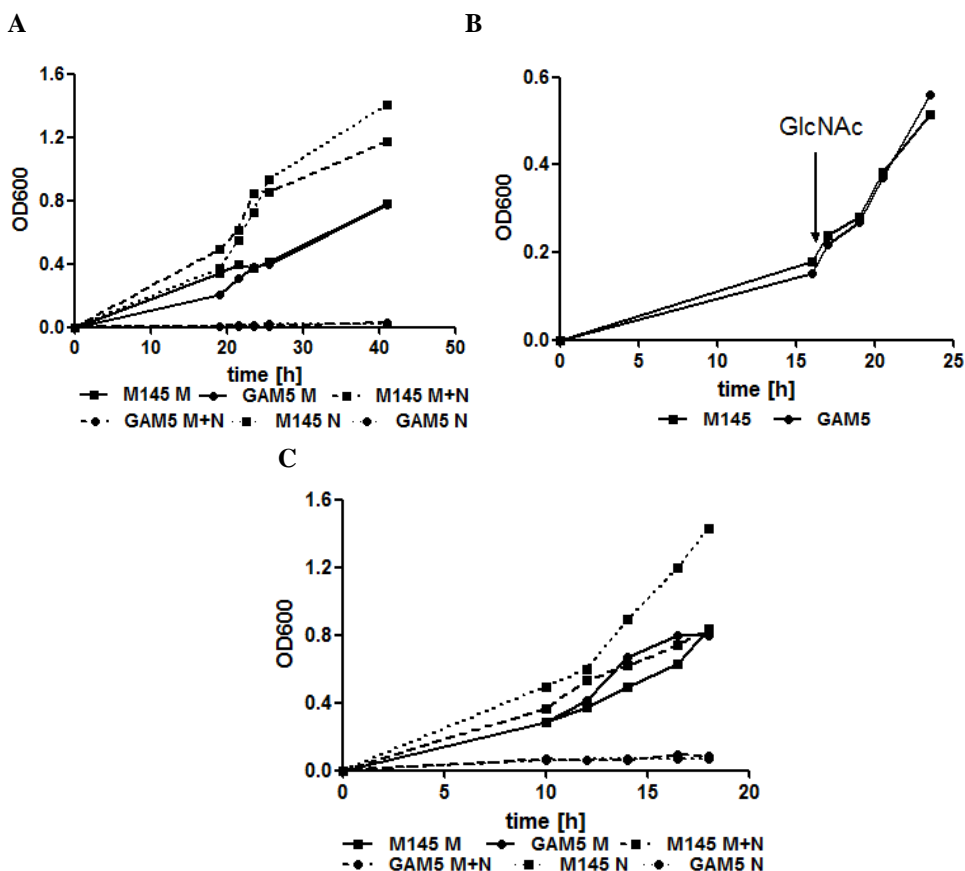


Figure 3. Effect of GlcNAc on growth of the *nagB* mutant.

A. Effect of GlcNAc on growth of *S. coelicolor* A3(2) M145 (■) and its *nagB* null mutant GAM5 (●). Strains were grown in liquid MM supplemented with either mannitol (50 mM) (M, solid line), GlcNAc (25 mM) (N, dashed line) or mannitol + GlcNAc (M+N, dotted line). **B.** Effect of GlcNAc induction on growth of *S. coelicolor* A3(2) M145 (■) and its *nagB* null mutant GAM5 (●). Strains were grown in liquid NMMP supplemented with mannitol (1% w/v), followed by the addition of 25 mM GlcNAc to the cultures at an OD₆₀₀ ~ 0.2. The addition of GlcNAc is indicated with an arrow. **C.** Same as (A), but now with spores that were pregerminated for 8 h in 2xYT at 30°C.

The *nagA* mutant GAM4 grew with a similar doubling time ($T_d \sim 3$ h) as the parent M145 in liquid-grown MM cultures in the presence of mannitol, but it reproducibly reached higher biomass levels (Fig. 4). Conversely, in MM with GlcNAc the doubling time of *nagA* mutants was much lower ($T_d \sim 5$ h) as compared to the parent for M145 ($T_d \sim 2$ h). This suggests that the likely accumulation of GlcNAc-6P impairs growth of *nagA* mutants, but the effect is not as dramatic as the accumulation of GlcN-6P in *nagB* mutants.

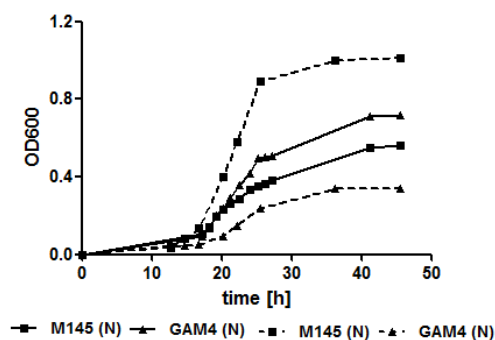


Figure 4. Effect of GlcNAc on growth of the *nagA* mutant.

Effect of GlcNAc on growth of *S. coelicolor* A3(2) M145(■) and its *nagA* null mutant GAM4 (●). Strains were grown in liquid NMMP supplemented with either mannitol (50 mM) (M, solid line) or *N*-acetylglucosamine (25 mM) (N, dashed line). Doubling times were derived from the linear part of the growth curves.

Effect of GlcNAc on development and antibiotic production of the *nagA* and *nagB* mutants in solid-grown cultures

The *nagA* and *nagB* mutants and the *nagAB* double mutant were similar to that of the parental strain in terms of colony morphology when grown on SFM, R5⁻ or MM agar plates supplemented with glucose, fructose, galactose, glycerol, maltose, mannitol, mannose, or xylose as the sole carbon source (Supplemental Fig. S1). However, major differences were observed when GlcNAc was added to the media. The toxicity of GlcNAc to *nagB* mutants in liquid-grown cultures was also observed on solid media, with *nagB* null mutants failing to grow on MM agar plates supplemented with 25 mM GlcNAc (Fig. 5A), while very poor growth was observed on R5 agar plates with GlcNAc (Fig. 5B). *nagA* mutants showed normal growth and development on MM agar plates with mannitol, while GlcNAc resulted in impaired growth, although some aerial hyphae were

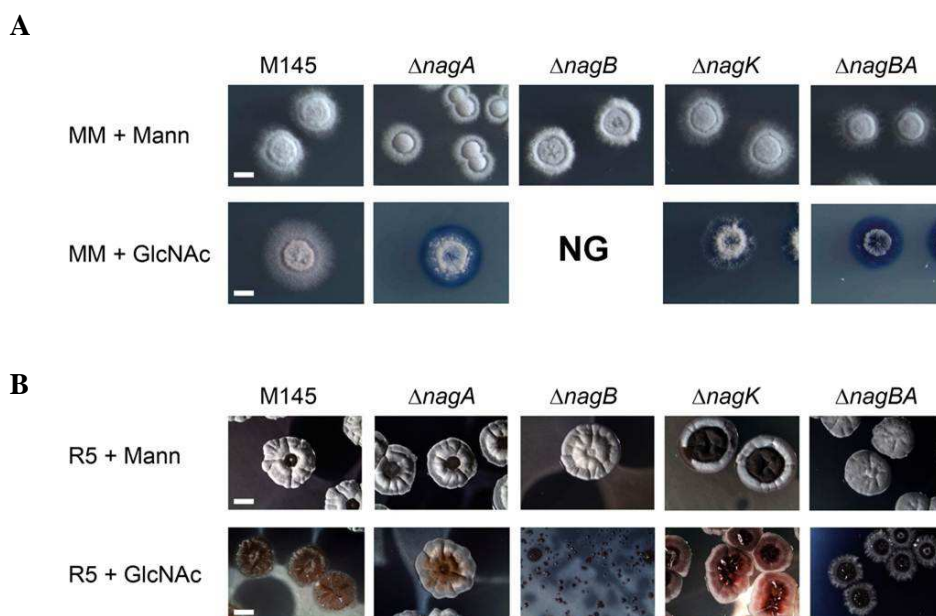


Figure 5. Phenotypic analysis of the *nag* mutants. Phenotypes of *S. coelicolor* M145 and its *nagA*, *nagB*, *nagK*, *nagAB* mutants (designated GAM4, GAM5, GAM6 and GAM9, respectively) were analyzed by stereomicroscopy. Colonies were grown for five days on MM (A) or R5 (B) agar plates, either with mannitol (top) or GlcNAc (bottom). For phenotypes of the strains on other media see Supplemental Fig. S1. Note that *nagB* mutants fail to grow (NG) on MM supplemented with GlcNAc, while on R5 with GlcNAc *nagB* mutants only produced a very thin layer of biomass. For complementation of the *nagA* and *nagB* mutants see Fig. S3.

formed. Interestingly, while GlcNAc was highly toxic to *nagB* null mutants on R5 agar plates supplemented with GlcNAc, the *nagA* null mutant GAM4 was able to enter development under these conditions (Fig. 5B), a phenotype that is similar to that of mutants lacking the GlcNAc transporter gene *nagE2* (Nothhaft *et al.*, 2010). In line with the idea that GlcN-6P accumulation causes toxicity to *nagB* null mutants grown on GlcNAc, the double mutant GAM9 (M145 $\Delta nagAB$) had a phenotype that was very similar to that of *nagA* mutants, with impaired growth on MM with GlcNAc and normal development on R5 agar plates with GlcNAc (Fig. 5). This is most likely due to the fact that the absence of *nagA* prevents the accumulation of GlcN-6P and thus toxicity of GlcNAc to *nagB* mutants.

The ability of the mutants to produce the pigmented antibiotics prodigiosine (Red) and actinorhodin (Act) was assessed in detail on R2YE agar plates. Since Red

production is switched on earlier than Act production (Bibb, 2005), antibiotic production was measured at different time points, namely after 42 h of growth (for Red production just prior Act biosynthesis) and after 48 h and 120 h for early and late Act production, respectively. Deletion of *nagA* only caused a minor reduction of Red production (about 25%) while deletion of *nagB* resulted in a 2.5-fold increase of prodiginine biosynthesis (Fig. 6A). Both deletions had a more drastic effect on Act production resulting in earlier and higher production with a 7- and 25-fold increase of Act biosynthesis after 48 h of growth for *nagA* and *nagB* mutants, respectively (Fig. 6B). After 120 h of growth all mutants showed similar excess of Act biosynthesis compared to the parental strain *S. coelicolor* M145 (increase of around 13-fold; Fig. S2). In contrast, *nagB* null mutant GAM5 formed extremely small colonies, with around 40% reduction of Red production and complete inhibition of extracellular Act production in the presence of GlcNAc (Fig. 6). After prolonged incubation (120 h) *nagB* null mutant GAM5 accumulated large amounts of intracellular Act on R5 supplemented with GlcNAc (Fig. S2).

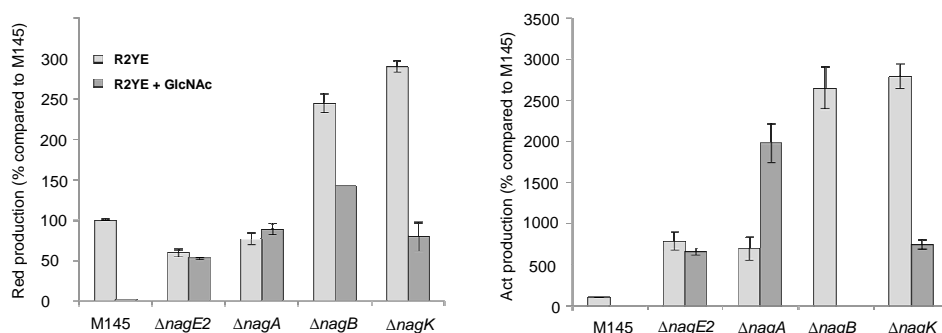


Figure 6. Quantification of antibiotic production. Production of prodiginines (top) or actinorhodin (bottom) was quantified relative to the production by the parental strain *S. coelicolor* M145 (which was set to 100%). Cultures were grown for 42 h (Red) or 48 h (Act) on R2YE agar plates with (dark bars) or without (light bars) GlcNAc. For 120 h see Fig. S2.

In a control experiment, the *nagA* and *nagB* gene replacement and IFD mutants were complemented with the low-copy vector pHJL401 (Larson & Hershberger, 1986) harboring the corresponding *nag* gene and its native promoter. *nagA* mutants GAM1 and GAM4 were complemented with pGAM5 (pHJL401/*nagKA*) and *nagB* mutants GAM2 and GAM5 with pGAM6 (pHJL401/*nagB*). The *nagKA* operon was used for complementation of *nagA* mutants to allow expression from the operon promoter.

Growth on MM and R5 agar plates with and without GlcNAc demonstrated that the complemented mutants had normal growth and GlcNAc sensing, underlining that the defects in growth and development in response to GlcNAc were indeed specifically due to the deletion of the respective *nag* genes (Fig. S3). Specifically, toxicity of GlcNAc to *nagB* mutants was relieved on both media, and GlcNAc sensing restored to both *nagA* and *nagB* mutants (e.g. bald phenotype and blocked antibiotic production on R5 with GlcNAc).

Effect of the deletion of *nagK*

The sugar kinase NagK catalyzes the phosphorylation of GlcNAc to GlcNAc-6P and the chromosomal deletion of *nagK* was performed as described previously for *nagA* and *nagB* mutants (see Materials and Methods section for details). We previously showed that transport of GlcNAc is mediated via the PTS in *S. coelicolor* (Nothaft *et al.*, 2010). If GlcNAc is exclusively transported via the PTS, the only internal source of GlcNAc is derived from the cell wall dismantling during programmed cell death (PCD) or chitin degradation providing chitooligosaccharides ((GlcNAc)_n, e.g. (GlcNAc)₂ and (GlcNAc)₃; Fig. 1B). When grown on rich medium agar plates the *nagK* mutant presented a 3- and 27-fold increased Red and Act production compared to the parental strain M145. Interestingly, on R2YE agar plates with GlcNAc the *nagK* mutant showed partial loss of the GlcNAc repressing effect that we could quantify to about 75% of the wild-type GlcNAc-mediated repression. This suggests that GlcNAc may be internalized in a PTS-independent manner under these growth conditions. As expected, the additional deletion of *nagK* did not significantly alter the morphology of the *nagA*, *nagB* or *nagAB* mutants on any of the media conditions tested (data not shown).

DISCUSSION

The aminosugar *N*-acetylglucosamine (GlcNAc) is a major carbon and nitrogen source for *Streptomyces*, which contributes to both cell-wall synthesis and primary metabolism, but also plays an important role as developmental signalling molecule (Nothaft *et al.*, 2003; Rigali *et al.*, 2008). The signalling cascade from nutrient sensing to development and antibiotic production is a highly complex process, based on cooperative interaction between signalling molecules, a phosphorylation state of the PTS, global and pathway-

specific regulators and their effector molecules. We previously demonstrated that GlcNAc acts as a signalling molecule that controls the onset of development and antibiotic production (Rigali *et al.*, 2006; Rigali *et al.*, 2008). Higher concentrations of GlcNAc outside the cell lock *Streptomyces coelicolor* in the vegetative growth phase under rich growth conditions (*feast*), but activate development and antibiotic production under poor conditions (*famine*). This principle has been applied successfully to enhance the expression of antibiotic biosynthetic gene clusters, including the clusters for Act, Red and the cryptic polyketide Cpk (Rigali *et al.*, 2008). The GntR regulator DasR acts as a responsive nutrient sensor, which has a pleiotropic regulon and among others represses *nag* metabolic genes, chitinolytic genes and the pathway-specific activator genes for antibiotic production (Colson *et al.*, 2007; Nazari *et al.*, 2011; Rigali *et al.*, 2006; Rigali *et al.*, 2008). Since the repressing activity of DasR is relieved allosterically by the effector molecule GlcN-6P (Rigali *et al.*, 2006), it follows that controlling the flux of GlcNAc may be a promising approach for metabolic engineering relating to improved screening of novel antimicrobial compounds.

From analysis of aminosugar metabolism and connected pathways (Fig. 1B) it follows that during growth on GlcNAc, *nagA* null mutants likely accumulate GlcNAc-6P and *nagB* null mutants likely accumulate GlcN-6P. Indeed, in line with the requirement of NagA for the production of the signalling molecule GlcN-6P, *nagA* null mutants had lost GlcNAc sensing. This underpins the current model of a direct signalling pathway from external GlcNAc to the accumulation of GlcN-6P, which then acts as allosteric effector of the developmental regulator DasR. However, when grown on GlcNAc, *nagA* null mutants likely accumulate large amounts of GlcNAc-6P, which in *E. coli* has two important regulatory roles, namely as allosteric activator for NagB (Calcagno *et al.*, 1984) and as effector molecule for NagC, the repressor of the *nag* regulon. In *E. coli*, inactivation of *nagA* (and hence accumulation of GlcNAc-6P) thus evokes derepression of the *nag* regulon (Plumbridge, 2009; Plumbridge, 1991). An additional effect is cell lysis, suggesting moderate toxicity of the accumulation of GlcNAc-6P to *E. coli* (White, 1968). Similar observations were made for *nagA* mutants in *Staphylococcus aureus* or *Gluconacetobacter xylinus*, which showed strongly reduced growth rates in the presence of GlcNAc (Komatsuzawa *et al.*, 2004; Yadav *et al.*, 2011). Indeed, we also found growth reduction for *nagA* null mutants of *S. coelicolor* in liquid minimal media with

GlcNAc, and the negative effect of GlcNAc on growth of the *nagA* mutant was shown by microscopy.

The accumulation of GlcN-6P is toxic to *S. coelicolor*, as demonstrated by the inability of *nagB* mutants to grow on GlcNAc. This toxicity was relieved by the additional deletion of *nagA* or the complete *nagKA* operon (Δ *nagABK*), and could also be complemented by re-introducing *nagB* on a low-copy vector. Interestingly, exponentially growing cells of *nagB* mutants had overcome the sensitivity to GlcNAc, as addition of GlcNAc during early logarithmic growth (OD₆₀₀~0.2) did not lead to growth inhibition. In contrast, prolonged germination of the spores, which also resulted in the formation of many young vegetative hyphae, did not relieve the sensitivity. This strongly suggests that in particular young vegetative hyphae are sensitive to the accumulation of GlcN-6P, perhaps because alternative ways to reduce the GlcN-6P pool are not yet active enough. GlcN-6P occupies a central position between cell-wall synthesis and glycolysis, and besides being converted to Fru-6P by NagB, it is also incorporated into murein following its conversion to UDP-GlcNAc by the action of GlmM (phosphoglucosamine mutase) and GlmU (N-acetylglucosamine-1-phosphate uridylyltransferase) (Fig. 1B) (Jolly *et al.*, 1997; Mengin-Lecreulx & van Heijenoort, 1994). In the absence of NagB, the major route to deplete GlcN-6P is incorporation into murein. Cell-wall synthesis exclusively takes place at the apical sites (Flårdh, 2003; Gray *et al.*, 1990) and with very few growing tips during early growth there may not be sufficient cell-wall synthesis to convert sufficient amounts of GlcN-6P, with as result the net accumulation of large amounts of this toxic metabolite. An alternative explanation would be lower enzymatic activity of GlmM during early growth. In *E. coli* GlmM is activated by phosphorylation, either by autophosphorylation or by the Ser/Thr kinase StkP (Jolly *et al.*, 1999; Jolly *et al.*, 2000). It is yet unknown how GlmM is activated in streptomycetes.

Preliminary work investigating the role of the GlcNAc kinase NagK revealed that the addition of GlcNAc has a less profound effect on development and antibiotic production in rich media when the *nagK* gene is deleted. The effect of NagK on the DasR-mediated GlcNAc nutrient-sensing system suggests the accumulation of its substrate GlcNAc. GlcNAc is internalized via the PTS in *S. coelicolor* (Nothaft *et al.*, 2003; Nothaft *et al.*, 2010), the existence of another import system that may be active under specific growth conditions cannot be ruled out. One candidate is perhaps the ABC

transporter encoded by SCO6005-6007 in *S. coelicolor*, which is orthologous to the GlcNAc/chitobiose transport operon *ngcEFG* in *Streptomyces olivaceoviridis*, although the sequence similarity is low (the various gene products share 30-40% aa identity). Alternatively, the accumulated GlcNAc-6P (which is a labile molecule) may be hydrolyzed to GlcNAc, which is not toxic. In both cases, NagK would be required to produce GlcNAc-6P in order to allow formation of the DasR effector molecule GlcN-6P.

Interestingly, when challenged with GlcNAc, we readily obtained suppressor mutants of the *nagB* null mutant. This is similar to observations in other bacterial systems, where spontaneous second-site mutations relieved the toxicity of accumulated sugar phosphates in *nagB* mutants (Plumbridge, 2009; White, 1968). Interestingly, when the *nagB* mutant spores were plated at high density onto MM agar plates containing GlcNAc, some colonies emerged with a frequency of around $1:10^5$, suggesting they had undergone spontaneous suppressor mutations to render the colonies insensitive to the toxicity of GlcNAc. Likely candidates for suppressor mutations include the GlcNAc-specific transporter genes *nagE2* and *nagF* and the metabolic genes *nagA* and *nagK*, but analysis of 16 independent suppressor mutants did not reveal changes in these genes or their promoter regions. We are currently analyzing the genomes of a series of the obtained suppressor mutants, and following re-creating the mutations in *nagB* mutants this will reveal which genes have undergone mutations, which will shed important new light on the metabolism of GlcNAc in *Streptomyces*.

Acknowledgements

We are grateful to Andriy Luzhetskyy for providing pUWLcre and for discussions and to Fritz Titgemeyer for discussions. SR is a research associate of the FRS-FNRS. This work is supported by a FRIA fellowship from the FRS-FNRS to ET, Grant R.CFRA.1237 from the Fonds Spéciaux of the University of Liège, and a VICI grant from the Netherlands Scientific Research council (NWO) to GPvW.

